

Discovering new CDK2 inhibitors by molecular docking and drug-likeness-based virtual screening for potential anticancer uses.

Mahmoud S. Elkotamy^{1,*}, Mohamed K. Elgohary¹, Islam A. Elkelesh¹, Abdallah M. Hamdy^{1,*}

¹Pharmaceutical Chemistry Department, Faculty of Pharmacy, Egyptian Russian University, Badr City, Cairo 11829, Egypt.

*Corresponding authors: Mahmoud S. Elkotamy, E-mail: mahmoud-elkotamy@eru.edu.eg, Abdallah M. Hamdy, E-mail: abdallahmohammed84@yahoo.com.

Received 31st December 2023, Revised 11th February 2024, Accepted 25th April 2024.

DOI: 10.21608/erurj.2024.259776.1106

ABSTRACT

Worldwide, cancer ranks as the second most lethal disease. There are several potential anticancer therapeutic targets, but CDK2 stands out. Not many third-generation CDK2 inhibitors targeting the kinase domain have made it to market yet, but there are plenty of first- and second-generation inhibitors on the market. Unfortunately, many of these drugs cause significant toxicity. In this study, we want to find new kinase inhibitors in the ZINC database that can block CDK2. This is why the ZINC database search, which is based on pharmacophores, and in-silico studies (ADMET, physicochemical, and drug-likeness) prediction has been used. Two active hits (**ZINC89856030** and **ZINC89867375**) were found using a series of virtual screening analyses. Out of the two, **ZINC89856030** exhibits the highest number of interactions inside the binding pocket, with a binding energy of -9.8 Kcal/mol. Both compounds showed promise as anticancer agents and as possible CDK2 inhibitors in the study and can be used for further assessment in vitro analysis to confirm their potentiality.

Keywords: Molecular docking; CDK2 inhibitors; Pharmacophore; ZINC database; Cancer.

1- Introduction

An increasingly pressing issue in global public health, cancer is a complicated and multi-dimensional disease. It has a significant impact on many populations, affecting millions of people annually and causing significant illness and death. Cancer epidemiology is an important public health and clinical management topic that seeks to understand the disease's prevalence, risk factors, and preventative strategies. With an eye toward providing a thorough introduction to cancer epidemiology, this section will focus on the field's worldwide influence, key risk factors, and noteworthy trends [1]. In 2020, an estimated 19.3 million new instances of cancer were detected, and the disease was directly responsible for almost 10 million deaths, according to the World Health Organization (WHO). These disturbing numbers highlight the critical need to make cancer prevention a top public health goal [2].

A cyclin-dependent kinase (CDK) is a family of proteins that is involved in many cellular functions and is essential for controlling the cell cycle. By coordinating signal transduction, gene expression, and enzymatic activities, cyclin-CDK complexes regulate cell cycle progression [3]. Association with CDK inhibitors, subcellular localization, stability, phosphorylation, and complex formation are all mechanisms that govern these complexes [4]. Because of their role in cell proliferation, CDKs play a significant role in the etiology of cancer and developmental diseases [5]. For cell division to occur, CDKs must provide a temporally organized phosphorylation sequence through hundreds of targets differently encoded at certain periods [6].

(CDK4) and (CDK6) correspondingly denotations for cyclin-dependent kinase 4 and cyclin-dependent kinase 6. These proteins have essential functions in controlling the cell cycle and other cellular processes. CDK4/6 inhibitors have demonstrated efficacy in the treatment of breast malignancies and are currently undergoing trials for other kinds of tumors [7]. Their mechanism of action involves inhibiting the phosphorylation of retinoblastoma protein (Rb) during the transition from G1 to S phase, effectively halting cell growth [8]. CDK4/6 inhibitors not only halt the growth of tumor cells in the G1 phase but also have broader impacts, resulting in the discovery of novel treatment possibilities [9, 10]. The FDA has authorized these inhibitors for treating progressed or advanced breast cancer that is hormone receptor-positive and HER2-negative [9]. In clinical oncology, resistance to CDK4/6 inhibitors presents a significant obstacle; consequently, ongoing research endeavours strive to elucidate the underlying mechanisms of resistance and devise effective countermeasures [11].

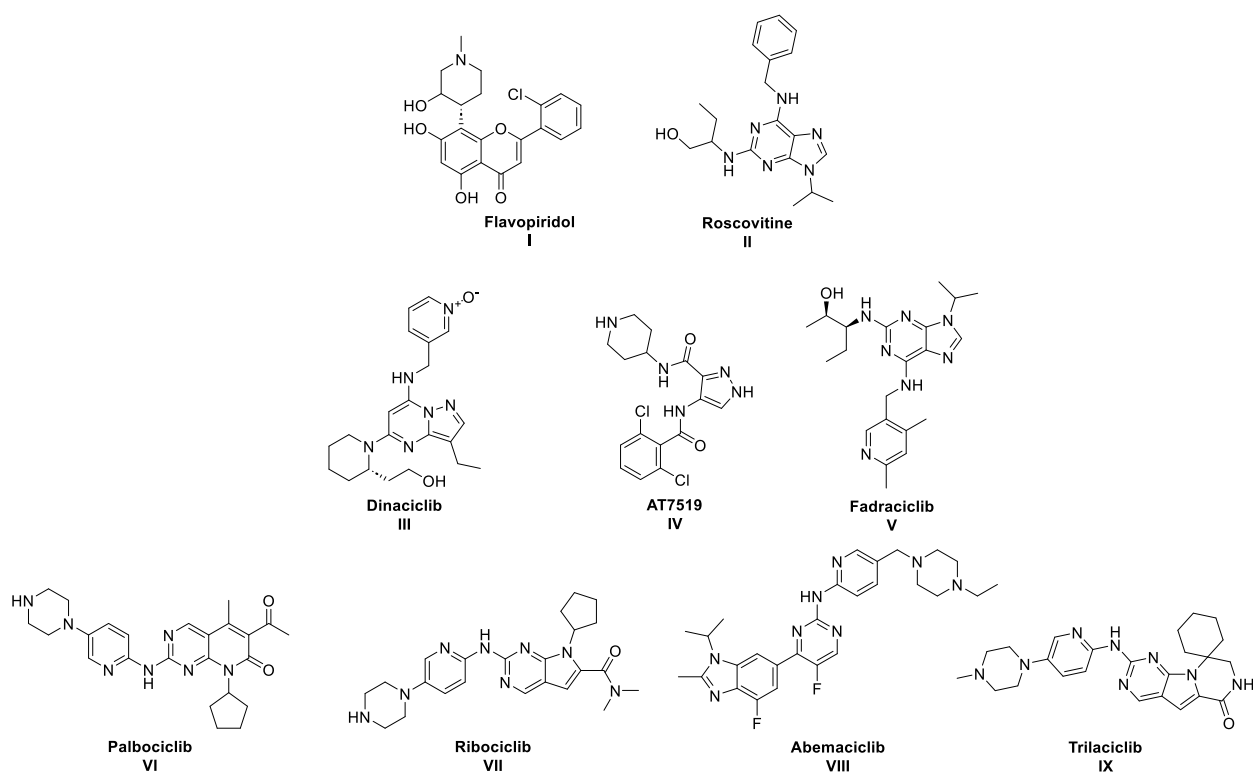


Fig. (1) Chart displaying the reported CDK inhibitors over time.

Flavopiridol and Roscovitine have been studied as cancer CDK inhibitors. Flavopiridol, a first-generation pan-CDK inhibitor, has shown promise in clinical studies and research. Studies have examined its effectiveness in numerous cancers and targets. CDK4/6 [12, 13]. Roscovitine, another first-generation pan-CDK inhibitor, has been extensively studied. Stages I and II clinical trials show inhibitory effects against numerous influenza strains. Virus strains have been detected. [14]. Roscovitine suppresses influenza A viruses, whereas Flavopiridol inhibits CDK4/6.

The CDK inhibitors Dinaciclib, AT7519, and Fadraciclib are in the same class. Through its effects on RNA pol II phosphorylation, the oncogenic marker MYC downregulation, and the anti-apoptotic protein MCL-1 upregulation, the pan-CDK inhibitor dinaciclib has demonstrated promise in lowering the development of medulloblastoma (MB) cells [15]. AT7519 is a small chemical multi-CDK inhibitor of the second generation that has shown promise as a glioblastoma multiforme (GBM) therapy. It hinders the development and survival of GBM cells, kills them through several mechanisms, and stops them from proliferating [13]. Another name for Fadraciclib is RGB-286638, an inhibitor of CDK4/6, CDK7, and CDK9. It is a second-generation CDK inhibitor. Its effectiveness in treating different forms of cancer has been studied and showed promise in clinical studies [16].

CDK inhibitors such as palbociclib, ribociclib, abemaciclib, and trilaciclib are used to treat cancer. They have demonstrated effectiveness in metastatic hormone receptor-positive, and HER2-negative breast cancer. Palbociclib, Ribociclib, and Abemaciclib are CDK4/6 inhibitors that the FDA has authorized. They have separate action mechanisms and resistance mechanisms [17].

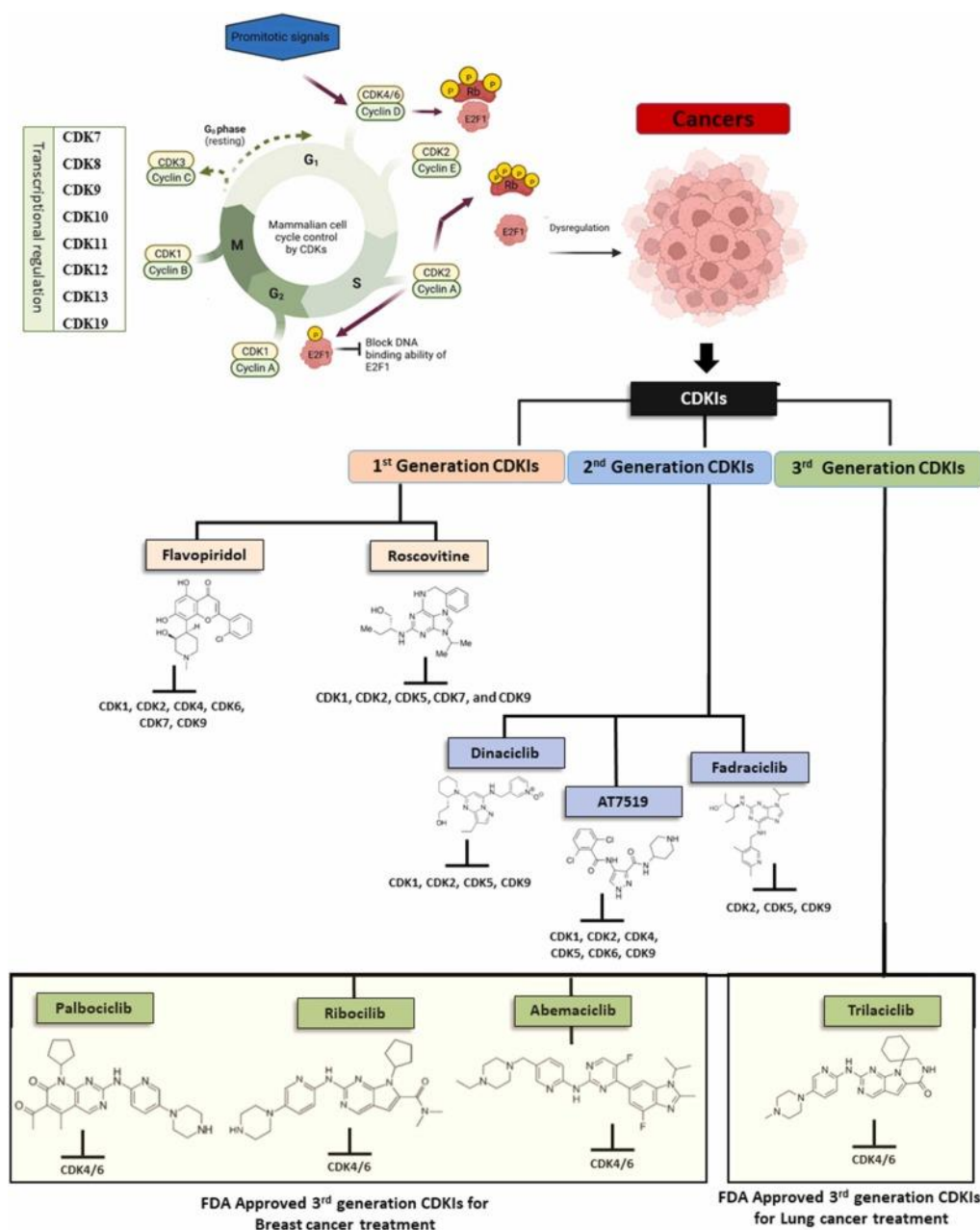


Fig. (2) An overview of the most studied first-, second-, and third-generation CDKIs, including their chemical structures and the key CDKs they target, that have been produced throughout the years [18].

Palbociclib and Abemaciclib's resistance mechanisms have been widely researched. Palbociclib-resistant breast cancer cells increase the expression of G2/M pathways and react to Abemaciclib. In contrast, Abemaciclib-resistant cells increase the expression of oxidative phosphorylation pathway mediators and respond to oxidative phosphorylation inhibitors [19]. Empirical data analysis has demonstrated that Palbociclib, Ribociclib, and Abemaciclib exhibit comparable effectiveness in terms of both progression-free survival and overall survival among patients diagnosed with estrogen and/or progesterone receptor-positive, HER2-negative metastatic breast cancer [20, 21]. Trilaciclib is a kind of medication known as a CDK4/6 inhibitor. It has demonstrated promise when used alongside chemotherapy in lowering the occurrence of myelosuppression, a side effect of chemotherapy [22].

The discovery of novel CDK inhibitors is vital in the field of cancer therapy due to the pivotal role CDKs play in governing the cell cycle, and their aberrant regulation is a characteristic feature of cancer [22, 23]. CDK inhibitors have demonstrated potential in suppressing the growth of cancer cells [24]. Initial CDK inhibitors had restricted selectivity and significant toxicity. However, recent progress in combination treatment has mitigated their adverse effects and toxicity, rendering them suitable for clinical use [18]. CDK inhibitors of the third generation have shown the most promising outcomes and are presently undergoing advanced clinical studies for the treatment of various types of cancer. The potential of these novel CDK inhibitors to transform conventional treatment approaches and offer unique therapeutic protocols for cancer patients is significant [25].

The main objective of drug discovery is finding a chemical that may alter the activity of a molecular target, often an enzyme or a receptor, that controls a disease-related biological process. One common way to conduct *in silico* techniques is by using virtual screening to look for potential compounds and hits. After analysis, the hits are often grouped into several structural groups. Additional chemical investigation is carried out on the clusters that show promise and have outstanding physicochemical qualities to produce the lead compound of the series. Computer-Aided Drug Design (CADD) is a new field with tremendous potential and closely related to computational chemistry. It was born out of the need to use computational modelling to predict the characteristics and activities of different compounds throughout the drug discovery process. The *in-silico* creation of novel, effective molecules can mitigate the enormous expense of experimental research in medication development. In rational drug design, CADD is an integral component that has become an indispensable technique for finding new compounds with desired pharmacological characteristics. Research into rational drug design with the hope of identifying a lead chemical is a rapidly growing field [26].

Because of this, finding new, less toxic CDK2 inhibitors quickly is of the utmost importance. The main objective of this study is to identify new CDK2 inhibitors by employing in-silico approaches. A search of the ZINC database yields numerous safe and effective CDK2 inhibitors that account for the pharmacophoric traits of the previously mentioned nine standard first-, second-, and third-generation inhibitors. This is achieved by using molecular docking, drug-likeness study, ADMET profiling, in-silico, and bioactivity analysis details of the top hit molecules.

2- Materials and methods

2.1. Finding and testing hits in a database using ligand-based pharmacophore mapping

2.1.1. The standards preparation and alignment

The nine standard molecules used in this study are as follows: Flavopiridol, Roscovitine, Dinaciclib, AT7519, Fadraciclib, Palbociclib, Ribociclib, Abemaciclib, and Trilaciclib. As indicated above, several of these compounds are third-generation inhibitors targeting the CDK4/6 domain, and they are now being tested in clinical trials as dual CDK4/CDK6 inhibitors targeting many malignancies. Using the Molecular Operating Environment (MOE v. 2022.09), the compounds were aligned and their shared pharmacophoric characteristics were mapped.

2.1.2. Pharmacophore query establishment

In this pharmacophoric analysis, hydrophobic areas, aromatic ring centers, metal ligators, hydrogen bond acceptors, and hydrogen bond donors were taken into account. Before using **Open Babel** to convert the molecules to a mol2 file format, they were sketched using **ACD ChemSketch** [27]. We proceeded to analyze the nine molecules whose alignment scores were the most negative value.

2.1.3. Virtual screening of the ZINC database depending on the obtained pharmacophore

Our second stop was at a different web server called "**ZincPharmer**" (<https://zincpharmer.csb.pitt.edu/>) [28], which included the prior output, which is now housed on this server. This web server used the **ZINC database** (<https://zinc.docking.org/>) to screen millions of compounds for those with almost identical pharmacophoric properties to the standard molecules. The database search returned a large number of hit molecules; however, only 20 molecules with an root mean square deviation (RMSD) value less than 0.15 were chosen for additional research. If RMSD between the output product and the input pharmacophores is small, then the two compounds are more closely related. According to a

recent paper, the study only took into account molecules with an RMSD cut-off value of less than 0.15 compared to the input pharmacophores.

2.2. Investigation of drug-likeness and analysis of molecular characteristics

By analyzing their chemical characteristics, we were able to determine whether or not each screened compound from the ZINC database was similar to a medication. Two web servers were utilized in this study: **SwissADME** (<https://www.swissadme.ch/>) and **admetSAR version 2.0** (<https://lmmd.ecust.edu.cn/admetsar2/>) [29, 30]. For both servers, the ligand compounds were entered using the SMILES format. We primarily utilized two well-established principles, namely Veber's rule and Lipinski's rule of five, for drug-likeness criteria. Each molecule in the ZINC database was analyzed based on many parameters, including molecular weight, octanol-water partition coefficient (log P), number of rotatable bonds, hydrogen bond donors and acceptors, and topological polar surface area (TPSA). In contrast to Veber's rule, which is concerned with the number of rotatable bonds (≤ 10) and TPSA ($\leq 140 \text{ \AA}^2$), Lipinski's rule of five addresses molecular weight ($\leq 500 \text{ Da}$), log P (≤ 5), hydrogen bond donors (≤ 5), and acceptors (≤ 10). The 3 drug-like compounds were ultimately rejected from further research due to violations of either of these two requirements leaving 17 compounds for further testing.

2.3. ADMET studies

Every molecule that made it through the drug-likeness screening was re-tested in ADMET trials to find out its pharmacokinetic profile and safety characteristics. The ADMET characteristics were determined using the admetSAR version 2.0 web server. Molecular structures were recorded after their upload in SMILES format. Several ADMET features, including as intestinal absorption, permeability of the blood-brain barrier, aqueous solubility, inhibition of P-glycoprotein and Cytochrome P-450, AMES mutagens, and carcinogenic potential, were evaluated for all of the drug-like compounds. We proceeded to choose the 5 safest molecules by ensuring that they maintained standard levels of all the parameters and showed minimal fluctuation compared to the reference compounds.

2.4. Preparation for molecular docking

2.4.1. Protein preparation

The research protein in question is the CDK2. The **RCSB protein data bank** (<https://www.rcsb.org/>) has the X-ray crystallographic structure of CDK2 protein with the inhibitor JWS648 co-crystallized with it (PDB ID: 3PXY) [31]. **Autodock 4.2.6 software** was first used to improve the protein via energy-minimization to a lower energy state. With the help of **MGL Tools version 1.5.6**, the protein was created. After dissolving the protein molecule to eliminate interference from water molecules, the co-crystal ligand was extracted to free up the

binding cavity. Before the addition of Gasteiger partial atomic charges, polar hydrogens were connected and bond ordering was determined. To make the protein compatible with Autodock 4, we added charges (Q) and changed the compatibility type to PDBQT, from PDB format.

2.4.2. Ligand preparation

Docking studies ligand preparation is performed on the 5 safest compounds with a decent pharmacokinetic profile and have passed the filters set by Lipinski's and Veber's rules. The ligands were represented using the **ACD ChemSketch program**. With the help of the **Discovery Studio 2021 visualizer**, these two-dimensional structures were transformed into three-dimensional models with the protein data bank (PDB) file extension. Utilizing **MGL Tools version 1.5.6**, we conducted ligand modelling. The program was updated to incorporate the ligands, and each molecule now has torsional degrees of freedom (torsdof). After that, each ligand is converted to PDBQT format by adding partial atomic charges (Q) using the Gasteiger-Marsili technique and making them compatible with Autodock 4 (T).

2.4.3. Validation of molecular docking system

Before investigating docking, the methods had to be validated. This protein's active site was redocked after removing the co-crystal ligand (JWS648) complexed with CDK2. Redocking study shows substantial co-crystal ligand-active site amino acid residue interaction.

2.4.4. Molecular docking studies

Autodock Vina was used to execute the docking [32]. To ensure successful docking interactions, minimal parameters were chosen for the docking investigations. A 60 X 60 X 60 grid-box with x, y, and z dimensions was established around the protein's active site region, with a spacing of 0.375 Å. The grid box's x, y, and z centers were adjusted to 64.436, 80.704, and -83.595, respectively, to determine the resolution. Nine conformers with substantial energy significance are produced by autodock vina. For any given ligand, the most active conformer is the one with the lowest docking score or binding energy. By comparing each of the test compounds to the nine reference standard molecules and then ranking the results by docking score, we were able to determine which compounds were the most active. **Autodock 4.2.6** was used to retrieve the docked complex in PDB format. BIOVIA Discovery Studio visualizer v.21 was utilized to analyze the docked complexes.

2.5. Bioactivity studies

Finding new CDK2 inhibitors is the primary goal of this research. As a result, finding out if the active compounds may inhibit enzymes and kinases is crucial. The major tool used for this is the **Molinspiration Cheminformatics v2020** web server, which can be accessed online at <https://www.molinspiration.com/>. Using the SMILES input format, this online server

conducted bioactivity investigations on all five of the safe and effective compounds that had previously undergone docking research. Using the premise that substances with higher bioactivity scores will have stronger pharmacological effects on the CDK2 enzyme, we narrowed the search down to two promising candidates.

3- Results and discussion

At first, the ZINC database search using the pharmacophore mapping of the nine standards returns several results out of the database's collection of several million molecules. Next, we separated 20 hit molecules with an RMSD less than 0.15 Å based on the lower RMSD values. Seventeen compounds were produced from these twenty hits after filtering them for drug-likeness using Lipinski's criterion and Veber's rule. Once again, they were run through a pharmacokinetic ADMET filter, narrowing the results to 5. Next, we conducted the molecular docking investigations and subsequently obtained two compounds. Two hit molecules were generated from these compounds after they were subjected to in-silico bioactivity tests that relied on kinase and enzyme inhibition, as CDK2 is considered to be both. The full virtual screening approach's pipeline is depicted in **Fig. 3**.

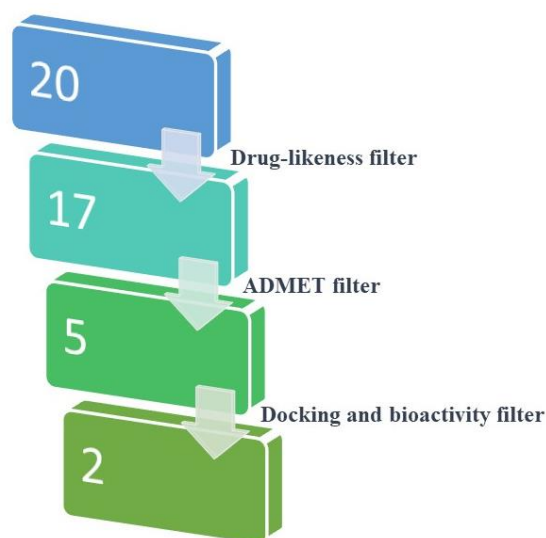


Fig. (3) The pipeline for the entire virtual screening method.

3.1. Pharmacophore mapping analysis

Important functional groups or structural features of a molecule are called pharmacophores. This molecule's agonistic or antagonistic biological action is owing to these components, which can bind to the active site residues of biological targets. The therapeutic benefits are enhanced in the end by this combination [33].

The nine standard molecules were aligned and their common pharmacophoric features extracted for pharmacophore mapping. ZincPharmer was enhanced with MOE v. 2022.09 pharmacophoric qualities before submitting the query. The website searches the Zinc database for similar pharmacophoric substances. Compounds with RMSD values between 0.11 and 0.15 will be prioritized during the search. The search stops when the number of results exceeds your query limit. Unweighted RMSD between the query and estimated orientation yields the result, while weighted RMSD computation determines hit orientation. All outputs will look like benchmarks. The compound search will stop if the number of hits exceeds the pharmacophoric characteristic range [28].

The alignment score of -84.3985 was determined as the highest among the nine molecules. After extracting the aligned molecules, the analysis yielded 5 spatial characteristics. The shared pharmacophoric characteristics were a hydrophobic area, an aromatic core, 3 metal ligators, 3 hydrogen bond acceptors, and a hydrogen bond donor. **Fig. 4** depicts the shared pharmacophoric characteristics of the nine standard compounds and an overlaid picture of all the standard molecules.

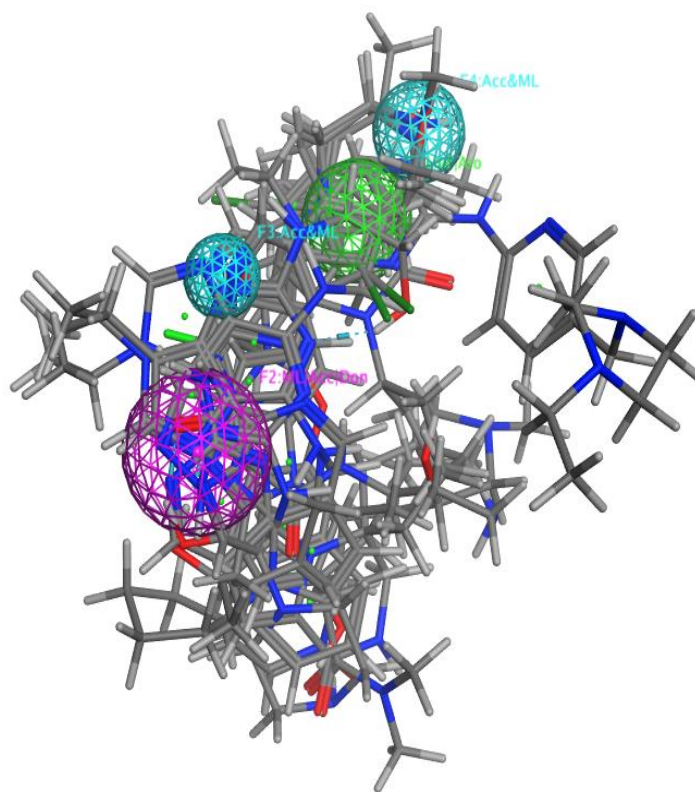


Fig. (4) Pharmacophore mapping was conducted on the nine standards to identify their shared pharmacophoric properties.

We ran these results through the ZINC database, which first returned 1,301,507 hits. However, we narrowed it down to 20 molecules with lower RMSD values ($<0.15 \text{ \AA}$), and these

molecules will be used for further in-silico investigations, ultimately leading to the generation of possible hit molecules. The 20 active compounds that were finalized from the ZINC database are included in **Table 1**, along with their RMSD values.

Table 1. Twenty active compounds and their root-mean-square (RMSD) values.

#	Compounds	RMSD values (Å)
1	ZINC17014677	0.11
2	ZINC16951980	0.11
3	ZINC89856012	0.11
4	ZINC89856030	0.12
5	ZINC89856839	0.12
6	ZINC89875969	0.12
7	ZINC89856850	0.12
8	ZINC89865781	0.13
9	ZINC17027418	0.13
10	ZINC89861513	0.13
11	ZINC89874788	0.13
12	ZINC89874811	0.14
13	ZINC37449257	0.14
14	ZINC36976167	0.14
15	ZINC37449112	0.14
16	ZINC89866417	0.15
17	ZINC84878582	0.15
18	ZINC89867375	0.15
19	ZINC37448905	0.15
20	ZINC89854169	0.15

Selection criteria: RMSD values should be < 0.15 Å.

3.2. Drug-likeness analysis

Many promising compounds never make it to clinical trials because they have an unsatisfactory pharmacokinetic profile and inferior drug-like qualities, even when they pass molecular docking. Because of this, identifying the drug-like compounds prior to docking

analysis is crucial. Its drug-likeness is one of the most important factors in determining a molecule's bioavailability and the likelihood of a successful lead development.

Drug-likeness is a key characteristic to examine throughout the early phases of drug discovery to ensure that a potential drug candidate has optimal bioavailability and can demonstrate high potency towards a biological target protein. We mostly utilized Lipinski's rule of five (RO5) and Veber's rule for the drug-likeness experiments [34, 35]. According to Lipinski's RO5, in order for a chemical to be considered a potential small molecule medicine, it has to meet certain requirements. These include having a molecular weight of 500 Da or less, an octanol-water partition coefficient (Log P) of 5 or less, or 10 or less hydrogen bond acceptors and 5 or fewer hydrogen bond donors. The primary idea behind Veber's rule is that a drug should have rotatable bonds of 10 or less and a topological polar surface area (TPSA) of 140 Å² or less in order for its oral bioavailability to be maximized.

A compound was removed from the actives pool if it violated either of the two rules. Molecules will diffuse and permeate more quickly with a smaller molecular weight [36]. The ability of a drug molecule to cross various lipophilic cell membranes and exert its effects depends on its solubility profile in both water and lipids; this is because the drug molecule will be transported through the bloodstream. Low water solubility and poor oral bioavailability are possible outcomes of a molecule's high lipophilicity, indicated by a Log P value greater than 5. Sequestration by highly lipophilic tissues can also lead to systemic toxicity. However, suppose the Log P value is less than 1. In that case, it will stay in the bloodstream without penetrating any cell membranes, leading to impaired intestinal and central nervous system permeability and decreased target specificity [37]. Given this, a value between 1 and 5 for Log P would be optimal.

To be eligible for consideration as a potentially game-changing small molecule in the drug discovery pipeline, a molecule must meet both Lipinski's and Veber's criteria and have an ALog P value between 1 and 5. In this case, this drug-likeness filter took into account all twenty hit compounds that were ordered from the ZINC database according to lower RMSD. A subset of the compounds were selected for additional investigation because they did not violate any of these conditions. The number of molecules was further reduced to 17 after this screening, and they were all subjected to ADMET profiling. **Table 2.** displays the drug-likeness features of the seventeen compounds that were ultimately selected.

Table 2. Characteristics of seventeen top hit compounds that resemble drugs.

Compound	Mol wt (g/mol)	Alog P	H-bond donors	H-bond acceptors	Lipinski's Rule	Rotatable bonds	TPSA (Å ²)	Veber's Rule
ZINC36976167	265.24	-0.27	1	6	No violation	4	102.79	No violation
ZINC37448905	291.3	0.62	1	5	No violation	3	121.8	No violation
ZINC37449112	266.23	-1.1	1	6	No violation	3	115.56	No violation
ZINC37449257	276.26	0.37	1	5	No violation	3	89.9	No violation
ZINC84878582	369.39	2.92	3	5	No violation	7	87.39	No violation
ZINC89854169	305.4	2.37	2	3	No violation	4	93.7	No violation
ZINC89861513	279.33	1.33	2	4	No violation	5	74.69	No violation
ZINC89866417	312.79	2.4	2	3	No violation	5	61.8	No violation
ZINC89867375	290.36	1.96	2	3	No violation	4	61.8	No violation
ZINC89874788	293.36	1.57	2	4	No violation	6	74.69	No violation
ZINC89874811	279.33	1.36	2	4	No violation	6	74.69	No violation
ZINC89856012	326.78	2.2	2	4	No violation	4	71.03	No violation
ZINC89856030	312.75	2	2	4	No violation	4	71.03	No violation
ZINC89856839	303.36	2.04	2	4	No violation	4	78.6	No violation
ZINC89856850	289.33	1.77	2	4	No violation	4	78.6	No violation
ZINC89865781	320.38	2.21	2	4	No violation	4	71.03	No violation
ZINC89875969	318.37	1.68	2	4	No violation	5	81.84	No violation

Standard criteria: Mol wt \leq 500 Da (g/mol); ALog P \leq 5 but not $<$ 1; H-bond donors \leq 5; H-bond acceptors \leq 10; Rotatable bonds \leq 10; TPSA \leq 140 Å².

3.3. ADMET profiling analysis

Absorption, distribution, metabolism, excretion, and toxicity (ADMET) evaluated many properties of the drugs, including their water solubility (Log S), gastrointestinal absorption, BBB penetrability, P-glycoprotein, also known as P-gp inhibition, and CYP450 isoenzyme inhibition [38].

The carcinogenic potential and mutagenicity of each hit molecule were assessed using AMES. A lipophilic barrier around the CNS is known as the blood-brain barrier (BBB). Medications that are able to cross the blood-brain barrier and exert their effects in the central nervous system are called CNS-targeting medicines.

Certain small-molecule kinase inhibitors must cross the blood-brain barrier (BBB) in order to target brain metastasis, glioblastomas, gliomas, and other brain tumors as well as CNS-related malignancies. Cancers can also develop in peripheral organs [39].

To increase oral bioavailability, molecules must undergo intestinal absorption in humans. This allows them to pass the intestinal lining and enter the systemic circulation [40]. In this case, intestinal absorption was a "positive" for every molecule. Drugs with low water solubility have a hard time making it into the bloodstream, which is a big issue in the medication development process.

Another essential metric for drug distribution is the Log S value [41]. Here is the quantitative Log S scale: insoluble for a value of -10, weakly soluble for a value of -6, soluble for a value of -4, very soluble for a value of -2, and very soluble for a value of 0. The ideal range for the Log S value is -4 to -2. All molecules are soluble because they all fall within the solvable range of -4 to -2.

A biological barrier known as P-glycoprotein (Permeability glycoprotein) limits the uptake of drugs into the brain and epithelial cells that pass through the intestinal lumen by acting as an efflux pump and exporting drug molecules and harmful xenobiotics outside the cell membrane [42].

Without P-gp inhibition, the blood-brain barrier (BBB) permeability decreases, making it more difficult for medications to act on the central nervous system (in this case, brain cancer), and metabolic liabilities rise, diminishing the effectiveness of some treatments.

To counteract potential toxicity, a modest dose of the medication may be administered due to the fact that high irreversible P-gp inhibition raises the drug concentration inside the cells. A key component of drug metabolism is CYP450 isoenzymes.

Five enzymes are known as cytochrome P450 (CYP) systems: CYP1A2, 2C19, 2C9, 2D6, and 3A4. Inhibiting CYP450 isoenzymes can slow metabolism, increase drug buildup

due to decreased renal clearance, and raise the risk of medication-drug interactions and other serious side effects [43]. We also considered the carcinogenicity and AMES mutagenicity of all the hit compounds to broaden the scope of the ADMET research. A molecule's mutagenic potential is represented by its AMES mutagenicity, which indicates the likelihood that it may induce genetic alterations within the body [44]. The carcinogenicity of a chemical is defined as its ability to cause cancer when tested independently. The molecules will be considered safest if they do not include any AMES toxins or carcinogens.

We screened 17 hit compounds using the aforementioned parameters; these molecules must adhere to the following ADMET filter requirements to be effective and safe. Following this ADMET filtering, only five hit compounds remained, which were further re-examined using molecular docking and bioactivity investigations to produce two hit molecules in docking and bioanalysis studies. The five hits' drug-likeness and ADMET characteristics are shown in **Table 3**.

Table 3. The five hits' drug-likeness and ADMET characteristics

Compound	Log S	Intestinal absorption	BBB penetration	P-gp inhibition	CYP450 inhibition					Ames mutagens	Carcinogens
					1A2	2C19	2C9	2D6	3A4		
ZINC89867375	-2.66	High	Yes	No	No	No	No	Yes	No	No	No
ZINC89856030	-3.03	High	Yes	No	Yes	No	No	Yes	No	No	No
ZINC89865781	-3.14	High	Yes	No	No	No	No	Yes	No	No	No
ZINC89856012	-3.2	High	Yes	No	No	No	No	Yes	No	No	No
ZINC89866417	-3.15	High	Yes	Yes	No	No	No	Yes	No	No	No

Standard criteria: Log S = -4 to -2; Intestinal absorption = positive; BBB penetration = positive; P-gp substrate = Yes/No; CYP450 inhibition= 'No' for at least 3 isoenzymes; Ames mutagens= 'No'; Carcinogens= 'No'.

3.4. Molecular docking analysis

The 'best-fit' posture between two molecules, in this case, a ligand and a protein, is determined by molecular docking, one of the virtual screening methods. Docking allows for a more accurate prediction of the optimal binding mode, which considers the energetic and

geometric conformation of a certain ligand within the target's active site and the binding's effectiveness, stability, and strength. The binding complex is considered more stable when the binding energy or docking score is negative [45]. Molecular docking investigation was conducted on the CDK2 protein (PDB ID: 3PXY) using five drug-like and safe compounds which are **ZINC89867375**, **ZINC89856030**, **ZINC89865781**, **ZINC89856012**, and **ZINC89866417**.

The redocked co-crystal conformer and its initial X-ray crystallographic conformation were determined to have a root mean square deviation (RMSD) value of 0.020 Å. Using Autodock Vina, validation shows that there are no noticeable noteworthy changes.

In docking studies, two parameters were considered: the minimum binding energy, and the total number of interactions between the ligand and receptor.

These interactions can be classified as hydrogen bonding, π interactions (π -cationic, π -anionic, π - π stacking, π -alkyl, π -sigma), Van der Waals interactions, and other hydrophobic interactions. In comparison to the original inhibitor JWS648, which had a binding energy of -8.0 kcal/mol, the five compounds **ZINC89856030**, **ZINC89867375**, **ZINC89856012**, **ZINC89865781**, and **ZINC89866417** had binding energies of -9.8, -9.0, -6.5, -6.7, and -8.0 kcal/mol, respectively. Additionally, within the binding pocket, **ZINC89856030**, **ZINC89867375**, **ZINC89856012**, **ZINC89865781**, and **ZINC89866417** made 8, 12, 7, 4 and 8 interactions, respectively, compared to JWS648's total of 9.

To select out the most active compounds from the five, we need an inhibitor with a lower binding energy and at least seven interactions in the binding site domain, as opposed to JWS648.

JWS648 (Fig. 5A) exhibited four hydrophobic interactions with the phenyl group and the amino acids Ile 10, Ala 31, Phe 82, and Leu 134. The triazine group demonstrated three hydrophobic interactions with Val 18, Leu 134, and Ala 144, as well as two hydrogen bonds with the nitrogen atom connected to the triazine with the amino acids Gln 131 and Asp 145.

ZINC89856030 (Fig. 5B) formed four alkyl hydrophobic interactions through its piperidine ring with the amino acids Ala 31, Leu 134, Val 64, and Ala 144. In addition to there was extra hydrogen bonding with the oxygen atom located on the piperidine ring with amino acid Phe 80. The benzo[1,3]dioxole ring exhibited two interactions: a π -alkyl interaction with Val 18 and a π -sigma interaction with Gly 11.

ZINC89867375 (Fig. 5C) exhibited a π -sigma interaction by means of its piperidine ring with the amino acid Ile 10. Furthermore, the oxygen atom that is bonded to the methyl group on the piperidine ring formed three contacts. Two of these interactions included

hydrogen bonding with the amino acids His 84 and Asp 86, while the third interaction was a van der Waals interaction with Lys 89. The chromane ring proved to be an optimal selection for the interaction, as it facilitated a total of 8 interactions. These interactions included alkyl interactions, as well as Pi-Pi stacking contacts and Pi-sigma interactions with amino acids Ala 31, Ala 144, Val 18, and Phe 82, Leu 134, Ile 10, respectively.

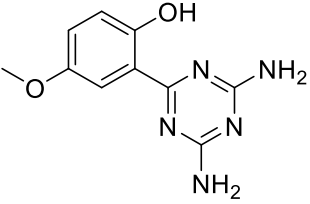
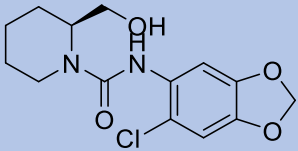
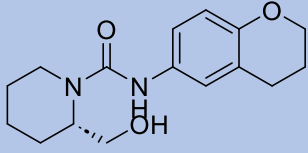
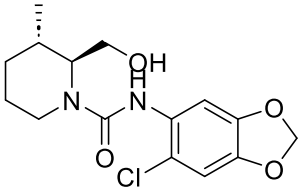
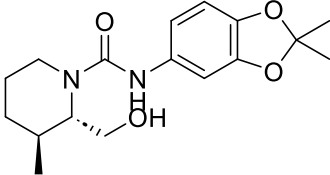
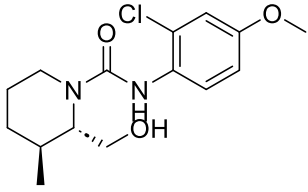
ZINC89856012 (**Fig. 5D**) demonstrated alkyl and Pi-sigma interactions with the phenyl group of benzo[1,3]dioxole. These interactions involved amino acids Pro 155 and Arg 36, respectively. Additionally, the chloro atom on the phenyl ring showed two alkyl interactions with Ile 35 and Phe 152. Thr 41 formed a hydrogen connection with the carbonyl group present in the molecule and van der Waals interactions with the oxygen atom connected to the piperidine ring.

ZINC89865781 (**Fig. 5E**) exhibited two alkyl interactions, one with its piperidine group and another with its phenyl group, specifically with amino acids Arg 200 and Arg 214, respectively. Leu 202 formed a hydrogen connection with the nitrogen atom present in the linker. The methyl group connected to the piperidine ring ultimately engaged in van der Waals interactions with Ala 201.

ZINC89866417 (**Fig. 5F**) exhibited five alkyl interactions with the piperidine ring, including the amino acids Ala 144, Val 18, Ala 31, Leu 134, and Phe 80. The oxygen group present on the methyl group linked to the piperidine ring exhibited hydrogen bonding with Glu 81. Ultimately, Ile 10 demonstrated two distinct interactions: the Pi-sigma interaction with the phenyl ring and the methyl group linked to the oxygen group on the phenyl ring.

Out of the five molecules considered for bioactivity investigations, two were determined to be active hits using molecular docking; these two compounds have the potential to inhibit CDK2 and so serve as anticancer medicines. With at least seven interactions, the two compounds that made it to the final round of hits have a strong binding affinity for CDK2. Their docking binding energies are even lower than those of the initial inhibitor, JWS648. Therefore, they can be developed as effective CDK2 inhibitors in the future due to their high affinity within the binding site domain.

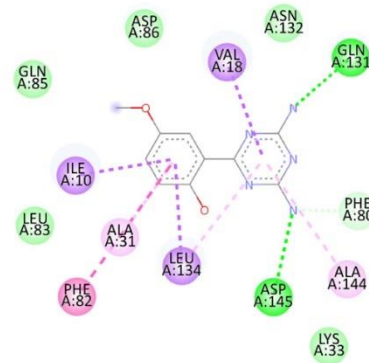
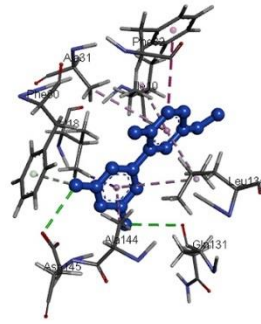
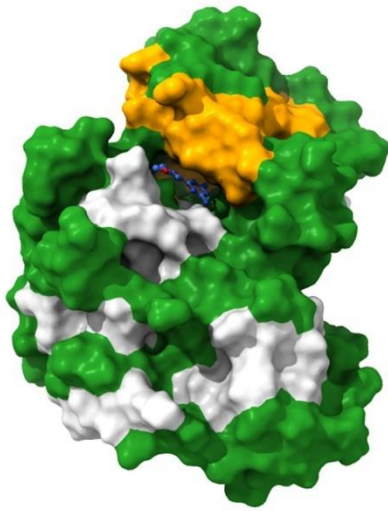
Table 4. includes the binding energies, total contacts, and interacting amino acid residues for the five hits and the original inhibitor co-crystallized with CDK2 protein JWS648.

Compounds	Structure	Binding energy (kcal/mol)	Total number of interactions	Interacting amino acid residues
JWS648		-8.0	9	ILE: 10, VAL: 18, ALA: 31, PHE: 82, LEU: 134, ALA: 144, ASP: 145
ZINC89856030		-9.8	8	GLY: 11, VAL: 18, ALA: 31, VAL: 64, LEU: 134, ALA: 144
ZINC89867375		-9.0	12	ILE: 10, VAL: 18, ALA: 31, PHE: 82, HIS: 84, ASP: 86, LEU: 134, ALA: 144
ZINC89856012		-6.5	7	ILE: 35, ARG: 36, THR: 41, PHE: 152, PRO: 155
ZINC89865781		-6.7	4	ARG: 200, LEU: 202, ARG: 214
ZINC89866417		-8.0	8	ILE: 10, VAL: 18, ALA: 31, PHE: 80, GLU: 81, LEU: 134, ALA: 144

Primary selection criteria: Binding energy < JWS648.

Secondary selection criteria: Total number of interactions ≥ 7 .

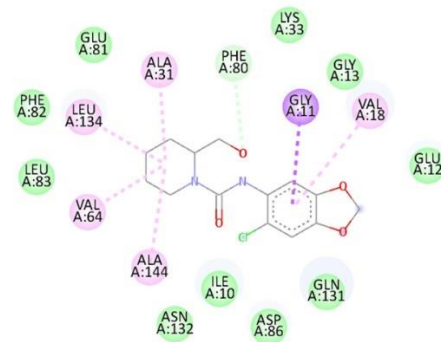
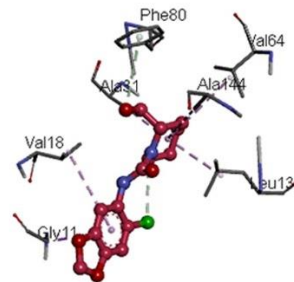
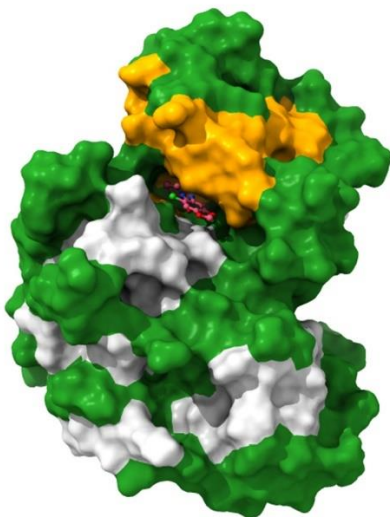
A]



Interactions

- van der Waals
- Conventional Hydrogen Bond
- Pi-Donor Hydrogen Bond
- Pi-Sigma
- Pi-Pi Stacked
- Pi-Alkyl

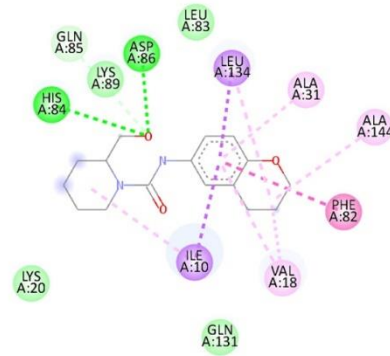
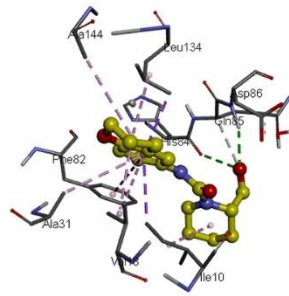
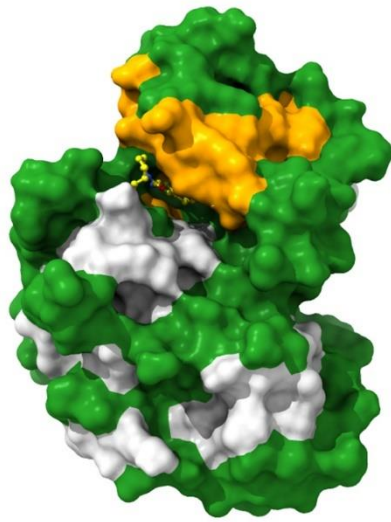
B]



Interactions

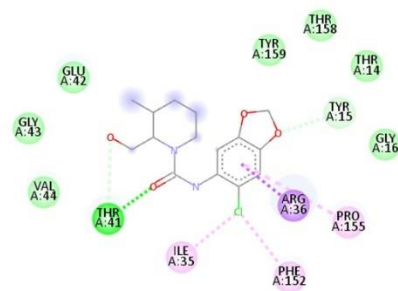
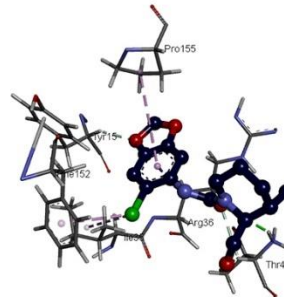
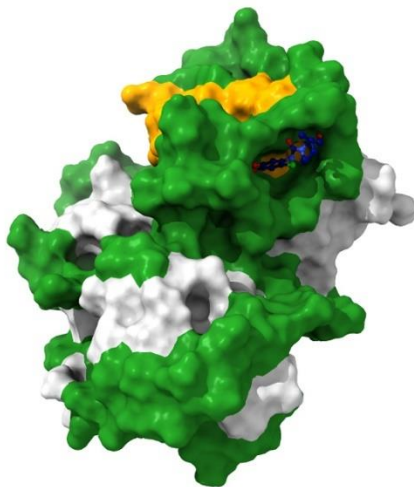
- van der Waals
- Pi-Donor Hydrogen Bond
- Pi-Sigma
- Alkyl
- Pi-Alkyl

C]



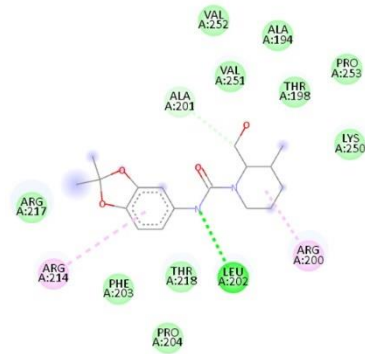
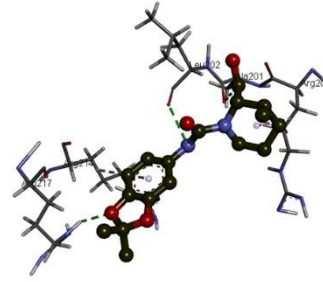
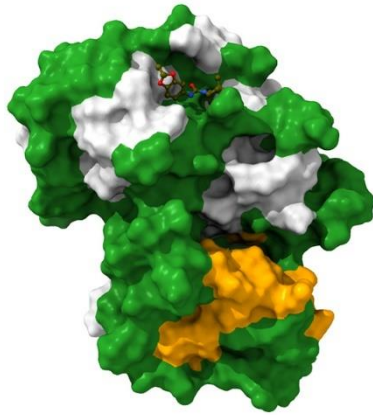
- Interactions**
- van der Waals
 - Conventional Hydrogen Bond
 - Carbon Hydrogen Bond
 - Pi-Sigma
 - Pi-Pi Stacked
 - Alkyl
 - Pi-Alkyl

D]



- Interactions**
- van der Waals
 - Conventional Hydrogen Bond
 - Carbon Hydrogen Bond
 - Pi-Sigma
 - Alkyl
 - Pi-Alkyl

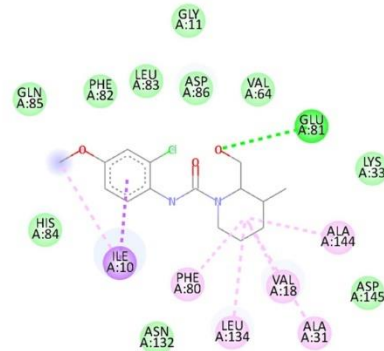
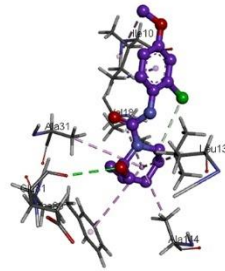
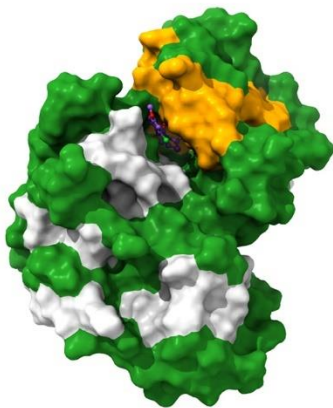
E]



Interactions

- van der Waals
- Conventional Hydrogen Bond
- Carbon Hydrogen Bond
- Alkyl
- Pi-Alkyl

F]



Interactions

- van der Waals
- Conventional Hydrogen Bond
- Pi-Sigma
- Alkyl
- Pi-Alkyl

Fig. (5) 2d and 3d interaction images of (A) JWS648, (B) ZINC89856030, (C) ZINC89867375, (D) ZINC89856012, (E) ZINC89865781 and (F) ZINC89866417, within the binding pocket of CDK2.

3.5. Bioactivity analysis

Here, kinase inhibition and enzyme inhibitory potential are the key factors in bioactivity research. Our main goal is to find compounds that can block CDK2. Since CDK2 is a kinase, it is important to determine if the active chemicals may block the activity of this protein. Since CDK2 is also an enzyme, it is of important to emphasize the inhibitory effects of all the compounds on this enzyme. A bioactivity score between 0.00 and 0.50 indicates the most inhibiting biological activity, a value between -0.50 and 0.00 suggests moderate activities, and a score below -0.50 is considered ineffective [46].

Table 5 shows the results of the bioactivity investigations that were conducted on the top two hit compounds and the JWS648, which pertain to their capacity to inhibit kinases and enzymes. With kinase and enzyme inhibition bioactivity scores of >0.00 , both compounds have demonstrated their efficacy as kinase and enzyme inhibitors against the CDK2 protein.

Table 5. Investigating the bioactivity of the two most successful compounds and JWS648 by inhibiting kinases and enzymes.

Compounds	Kinase Inhibitor	Enzyme Inhibitor
JWS648	0.10	0.31
ZINC89856030	0.13	0.10
ZINC89867375	0.15	0.25

Selection criteria: For enzyme and kinase inhibition, the bioactivity score should be greater than 0.00.

4- Conclusion

Of all the targets that have recently been the focus of anticancer drug development, CDK2 is crucial. Although several CDK2 inhibitors have entered clinical trials, none have been commercialized. Here, we obtained many powerful compounds from the ZINC database that can potentially be used as CDK2 inhibitors of the third generation. After searching the ZINC database for the common pharmacophoric properties, nine standard compounds were used in a pharmacophore mapping analysis, and twenty hit molecules were found. Out of all the compounds, the virtual screening method yielded two of the most powerful and effective molecules, ZINC89856030 and ZINC89867375. Out of the two, ZINC89856030 has the highest number of contacts with the CDK2 domain's binding pocket. Due to their potential strong CDK2 affinity and lack of adverse effects, these two bioactive compounds are deemed

safe for human use. The study's results will provide researchers with data that they may use as a starting point for optimizing leads as anticancer medicines that target CDK2. Next, we will assess the enzyme activity and conduct in-vitro studies using cancer cell lines. After that, we will move on to synthesize the final hit molecules.

- **Conflict of Interest**

The authors declare no conflict of interest.

5- References

1. Sung H, Ferlay J, Siegel RL, Laversanne M, Soerjomataram I, Jemal A, et al. Global Cancer Statistics 2020: GLOBOCAN Estimates of Incidence and Mortality Worldwide for 36 Cancers in 185 Countries. *CA Cancer J Clin.* 2021;71(3):209-49.
2. Leiter A, Veluswamy RR, Wisnivesky JP. The global burden of lung cancer: current status and future trends. *Nature Reviews Clinical Oncology.* 2023;20(9):624-39.
3. Rodger A, Marshall D. Beginners guide to circular dichroism. *Biochemist.* 2021;43(2):58-64.
4. Birnbaum M. A Circular Dichroism Analysis of Commercially Available Powdered Whey Protein Structure. *J Nutr Food Sci.* 2018;8(690):2.
5. Brooks G. Cyclins, cyclin-dependent kinases, and cyclin-dependent kinase inhibitors: detection methods and activity measurements. *Cell Cycle Control: Mechanisms and Protocols.* 2005:291-8.
6. Örd M, Möll K, Agerova A, Kivi R, Faustova I, Venta R, et al. Multisite phosphorylation code of CDK. *Nature structural & molecular biology.* 2019;26(7):649-58.
7. Zhang S, Xu Q, Sun W, Zhou J, Zhou J. Immunomodulatory effects of CDK4/6 inhibitors. *Biochimica et Biophysica Acta (BBA)-Reviews on Cancer.* 2023:188912.
8. Darmmikrobiota DH, zu von Dickdarmzellen P, von onkogenen Genen E. CDK4/6-Inhibitor plus Fulvestrant verlängert Überleben. *Deutsche Zeitschrift für Onkologie.* 2022;54:119-22.
9. Goel S, Bergholz JS, Zhao JJ. Targeting CDK4 and CDK6 in cancer. *Nature Reviews Cancer.* 2022;22(6):356-72.
10. Pang J, Li H, Sheng Y. CDK4/6 inhibitor resistance: A bibliometric analysis. *Frontiers in Oncology.* 2022;12:917707.
11. Knudsen ES, Witkiewicz AK. The Strange Case of CDK4/6 Inhibitors: Mechanisms, Resistance, and Combination Strategies. *Trends Cancer.* 2017;3(1):39-55.

12. Obakachi VA, Kehinde I, Kushwaha ND, Akinpelu OI, Kushwaha B, Merugu SR, et al. Structural based investigation of novel pyrazole-thiazole Hybrids as dual CDK-1 and CDK-2 inhibitors for cancer chemotherapy. *Molecular Simulation*. 2022;48(8):687-701.
13. Mounika P, Gurupadayya B, Kumar HY, Namitha B. An Overview of CDK Enzyme Inhibitors in Cancer Therapy. *Current Cancer Drug Targets*. 2023;23(8):603-19.
14. Zhang M, Zhang L, Hei R, Li X, Cai H, Wu X, et al. CDK inhibitors in cancer therapy, an overview of recent development. *American journal of cancer research*. 2021;11(5):1913.
15. Zhao W, Zhang L, Zhang Y, Jiang Z, Lu H, Xie Y, et al. The CDK inhibitor AT7519 inhibits human glioblastoma cell growth by inducing apoptosis, pyroptosis and cell cycle arrest. *Cell Death & Disease*. 2023;14(1):11.
16. Tsao A-N, Chuang Y-S, Lin Y-C, Su Y, Chao T-C. Dinaciclib inhibits the stemness of two subtypes of human breast cancer cells by targeting the FoxM1 and Hedgehog signaling pathway. *Oncology Reports*. 2022;47(5):1-12.
17. Zhu Z, Zhu Q. Differences in metabolic transport and resistance mechanisms of Abemaciclib, Palbociclib, and Ribociclib. *Frontiers in Pharmacology*. 2023;14.
18. Mughal MJ, Bhadresha K, Kwok HF, editors. CDK inhibitors from past to present: A new wave of cancer therapy. *Seminars in Cancer Biology*; 2023: Elsevier.
19. Navarro-Yepes J, Kettner NM, Rao X, Bishop CS, Bui TN, Wingate HF, et al. Abemaciclib is effective in palbociclib-resistant hormone receptor-positive metastatic breast cancers. *Cancer Research*. 2023;83(19):3264-83.
20. Cejuela M, Gil-Torrvalvo A, Castilla MÁ, Domínguez-Cejudo MÁ, Falcón A, Benavent M, et al. Abemaciclib, Palbociclib, and Ribociclib in Real-World Data: A Direct Comparison of First-Line Treatment for Endocrine-Receptor-Positive Metastatic Breast Cancer. *International Journal of Molecular Sciences*. 2023;24(10):8488.
21. Del Vecchio M, Pantano CL, Zelante F, Re B, Ladisa V. 5PSQ-059 Real-world clinical data of palbociclib and ribociclib in breast cancer patient. *British Medical Journal Publishing Group*; 2023.
22. Kahraman S, Erul E, Seyyar M, Gumusay O, Bayram E, Demirel BC, et al. Treatment efficacy of ribociclib or palbociclib plus letrozole in hormone receptor-positive/HER2-negative metastatic breast cancer. *Future Oncology*. 2023;19(10):727-36.
23. Gil-Gil M, Alba E, Gavilá J, de la Haba-Rodríguez J, Ciruelos E, Tolosa P, et al. The role of CDK4/6 inhibitors in early breast cancer. *The Breast*. 2021;58:160-9.
24. Abdelmalak M, Singh R, Anwer M, Ivanchenko P, Randhawa A, Ahmed M, et al. The renaissance of CDK inhibitors in breast cancer therapy: an update on clinical trials and therapy resistance. *Cancers*. 2022;14(21):5388.
25. Zhang M, Zhang L, Hei R, Li X, Cai H, Wu X, et al. CDK inhibitors in cancer therapy, an overview of recent development. *Am J Cancer Res*. 2021;11(5):1913-35.

26. Bagchi M. In Silico Evaluations of Activity/Toxicity Profiles of Chemotherapeutic Agents. *J Bioanal Biomed.* 2016;8:e140.
27. O'Boyle NM, Banck M, James CA, Morley C, Vandermeersch T, Hutchison GR. Open Babel: An open chemical toolbox. *Journal of cheminformatics.* 2011;3(1):1-14.
28. Koes DR, Camacho CJ. ZINCPharmer: pharmacophore search of the ZINC database. *Nucleic acids research.* 2012;40(W1):W409-W14.
29. Yang H, Lou C, Sun L, Li J, Cai Y, Wang Z, et al. admetSAR 2.0: web-service for prediction and optimization of chemical ADMET properties. *Bioinformatics.* 2019;35(6):1067-9.
30. Daina A, Michielin O, Zoete V. SwissADME: a free web tool to evaluate pharmacokinetics, drug-likeness and medicinal chemistry friendliness of small molecules. *Scientific reports.* 2017;7(1):42717.
31. Betzi S, Alam R, Martin M, Lubbers DJ, Han H, Jakkaraj SR, et al. Discovery of a Potential Allosteric Ligand Binding Site in CDK2. *ACS Chemical Biology.* 2011;6(5):492-501.
32. Trott O, Olson AJ. AutoDock Vina: improving the speed and accuracy of docking with a new scoring function, efficient optimization, and multithreading. *Journal of computational chemistry.* 2010;31(2):455-61.
33. Güner OF. Pharmacophore perception, development, and use in drug design: Internat'l University Line; 2000.
34. Lipinski CA, Lombardo F, Dominy BW, Feeney PJ. Experimental and computational approaches to estimate solubility and permeability in drug discovery and development settings. *Advanced drug delivery reviews.* 1997;23(1-3):3-25.
35. Veber DF, Johnson SR, Cheng H-Y, Smith BR, Ward KW, Kopple KD. Molecular properties that influence the oral bioavailability of drug candidates. *Journal of medicinal chemistry.* 2002;45(12):2615-23.
36. Waring MJ. Defining optimum lipophilicity and molecular weight ranges for drug candidates—molecular weight dependent lower log D limits based on permeability. *Bioorganic & medicinal chemistry letters.* 2009;19(10):2844-51.
37. Waring MJ. Lipophilicity in drug discovery. *Expert Opinion on Drug Discovery.* 2010;5(3):235-48.
38. da Silva Júnior OS, Franco CdJP, de Moraes AAB, Cruz JN, da Costa KS, do Nascimento LD, et al. In silico analyses of toxicity of the major constituents of essential oils from two Ipomoea L. species. *Toxicon.* 2021;195:111-8.
39. Heffron TP. Small molecule kinase inhibitors for the treatment of brain cancer. *Journal of medicinal chemistry.* 2016;59(22):10030-66.
40. Radchenko E, Dyabina A, Palyulin V, Zefirov N. Prediction of human intestinal absorption of drug compounds. *Russian Chemical Bulletin.* 2016;65:576-80.

41. Lipinski C. Poor aqueous solubility—an industry wide problem in drug discovery. *Am Pharm Rev.* 2002;5(3):82-5.
42. Lin JH, Yamazaki M. Role of P-glycoprotein in pharmacokinetics: clinical implications. *Clinical pharmacokinetics.* 2003;42:59-98.
43. Hollenberg PF. Characteristics and common properties of inhibitors, inducers, and activators of CYP enzymes. *Drug metabolism reviews.* 2002;34(1-2):17-35.
44. Mortelmans K, Zeiger E. The Ames Salmonella/microsome mutagenicity assay. *Mutation research/fundamental and molecular mechanisms of mutagenesis.* 2000;455(1-2):29-60.
45. Yuriev E, Agostino M, Ramsland PA. Challenges and advances in computational docking: 2009 in review. *Journal of Molecular Recognition.* 2011;24(2):149-64.
46. Arshad M, Shoeb Khan M, Asghar Nami S, Ahmad D. Synthesis, characterization, computational, antimicrobial screening, and MTT assay of thiazolidinone derivatives containing the indole and pyridine moieties. *Russian Journal of General Chemistry.* 2018;88:2154-62.